

# Chapter 7

## Computed Tomography Assessment of the Tricuspid Valve and the Right Heart



Saurav Uppal, Laurie Bossory, Michael Biersmith, and Thura T. Harfi

### Introduction

In recent years, there has been renewed interest in the assessment and management of tricuspid valve (TV) disease, particularly tricuspid regurgitation (TR). Moderate-to-severe TR affects nearly 1.6 million patients in the United States, and is independently associated with increased cardiac events and overall mortality [1–4]. The majority of TR is functional in nature, often occurring in the context of left-sided heart disease, atrial fibrillation, or pulmonary hypertension (PHTN). Untreated severe symptomatic TR carries a poor prognosis, even after accounting for left-sided valvulopathy and congenital heart disease (CHD) [5]. Along with the renewed interest in TV disease, there has also been a growing awareness of right ventricular (RV) function.

In addition to left ventricular dysfunction, both PHTN and congenital heart disease can lead to progressive RV dysfunction and TR. With the improvements in the management of heart failure, patients with left ventricular (LV) dysfunction are living longer and into more advanced stages of their disease. Similar trends have been noted in the PHTN and congenital heart disease populations, particularly with the emergence and growth of dedicated PHTN and adult-congenital heart disease

---

**Supplementary Information** The online version contains supplementary material available at [\[https://doi.org/10.1007/978-3-030-92046-3\\_7\]](https://doi.org/10.1007/978-3-030-92046-3_7).

---

S. Uppal · L. Bossory · M. Biersmith  
Department of Cardiovascular Medicine, The Ohio State University Wexner Medical Center,  
Columbus, OH, USA  
e-mail: [saurav.uppal@osumc.edu](mailto:saurav.uppal@osumc.edu); [kaurie.bossory@osumc.edu](mailto:kaurie.bossory@osumc.edu)

T. T. Harfi (✉)  
Department of Medicine, The Ohio State University Wexner Medical Center,  
Columbus, OH, USA  
e-mail: [thura.harfi@osumc.edu](mailto:thura.harfi@osumc.edu)

subspecialties. The prevalence of PHTN is estimated to be about 127 cases/100,000 population in 2012 based on a cohort study from Canada [6]. As of 2010, an estimated 2.4 million people have CHD in the United States, and this population continues to grow [7]. Though this increased survivorship is certainly commendable, there is a pressing need to better understand and mitigate the effects of progressive right heart failure often noted in these populations. Progressive RV dysfunction and dilation can lead to annular dilation of the TV causing TR. Many studies have shown that patients with RV dysfunction and severe TR tend to have worse outcomes [8–10]. Given the increasing prevalence of right-sided dysfunction and the correlation with clinical outcomes, it has become prudent to have better assessment of the RV and right-sided structures including the TV.

In this chapter we will discuss the utilization of multi-detector computed tomography (MDCT) as it relates to the assessment of RV function and TV and for planning various novel transcatheter TV interventions.

## **The Role of CT in the Assessment of the Right Heart: General Principles**

Given the resurging interest in TV disease, as well as the rapid evolution in transcatheter TV devices, high-fidelity imaging assessment of the right heart anatomy is paramount. The right heart—including the RV, right atrium (RA), TV, and tricuspid annulus (TA)—is notoriously difficult to image and quantify due to its complex geometry. There are several imaging modalities used to evaluate the right heart, each with their own strengths and weaknesses.

Traditionally, echocardiography, particularly transthoracic echocardiography (TTE), has been the standard imaging modality to evaluate both LV and RV function. Given its high temporal resolution, TTE provides a good assessment of valvular function and morphology. Advantages include wide accessibility, relatively low cost, noninvasive nature, excellent temporal resolution, and shorter length of exam. Despite these advantages, TTE can be limited by acoustic shadowing secondary to patient characteristics such as obesity, chronic obstructive pulmonary disease, and small intercostal spaces. Moreover, the complex geometry of the RV and the TV can make the assessment more challenging.

Cardiac magnetic resonance (CMR) imaging is the current standard for evaluation of the RV. Despite this, there are several shortcomings that preclude utilization of this imaging modality for all patient populations. Owing largely to expense, the accessibility of CMR has traditionally been limited to tertiary-care academic centers. Additional barriers include longer scan times, patient's claustrophobia, contrast limitations for patients with end-stage kidney disease, and safe and/or effective image acquisition in patients with metallic implantable devices such as pacemakers and defibrillators. Due to these limitations, MDCT has emerged as a valuable alternate imaging modality.

Multi-detector computed tomography has excellent spatial resolution that is superior to both echocardiography and CMR. Currently, MDCT has spatial resolution around 0.5 mm in the  $x$ ,  $y$ , and  $z$  axes, and continued improvements are expected with newer scanner technology. This is in contrast to CMR, which has a spatial resolution around 1–2 mm. High spatial resolution is one of the primary strengths of CT and is exceptionally useful in preprocedural planning for transcatheter valve therapies [11]. Claustrophobic patients can usually tolerate undergoing cardiac CT without difficulty. Additionally, with newer-generation cardiac CT scanners, the temporal resolution has improved significantly. For example, dual-source CT scanners can obtain images with a resolution <80–100 milliseconds [12]. Such advances have made it possible to obtain real-time evaluation of cardiac function, including ejection fractions of LV and RV. Furthermore, cardiac CT imaging is the only imaging modality that affords real 3D (or even 4D) datasets that provide multiplane reconstruction of images, which can facilitate procedural and surgical planning.

Although CMR is still considered the standard for left and right ventricular volume and ejection fraction measurements, cardiac CT offers accurate assessment of cardiac chambers comparable to CMR in a fraction of the time [13]. Studies have shown comparable assessment of ventricular function with CT compared to CMR [14]. MDCT is an imaging option for RV assessment in patients who have defibrillators or cardiac synchronization devices that are non-MRI compatible and offers an alternative for patients who struggle with anxiety or claustrophobia. The multi-society guidelines consider cardiac CT an appropriate test for evaluation of right and left heart function and structure [15].

Two important drawbacks of cardiac CT are the exposure to ionizing radiation and the use of iodinated contrast media, which are known to be nephrotoxic. Fortunately, the radiation exposure associated with cardiac CT has dramatically decreased over the past decade with newer generation CT scanners [16].

## **Utility of CT in Assessment of Right Heart**

### ***CT Acquisition Techniques to Optimize Right Heart Visualization***

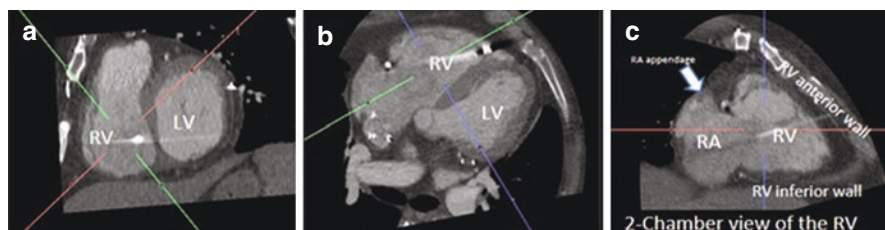
The traditional CT protocol for a coronary angiogram utilizes injection of contrast media followed by a saline bolus. This protocol results in optimal opacification of the left heart structures, but a varying degree of opacification of the right heart. Additionally, it leaves significant streaking artifact in the right atrium as the contrast from the superior vena cava (SVC) mixes with the blood coming from the inferior vena cava (IVC). In order to optimize left and right heart contrast opacification and avoid the streaking artifact in the RA, a triphasic contrast injection protocol is recommended. A triphasic contrast injection protocol includes a 60–65 ml of contrast media, followed by 20 ml of a 50–50 or 70–30 mixture of contrast–saline mixture

followed by a 40 ml saline flush. The recommended infusion rate is 5–6 ml per second. This protocol has been shown to optimize visualization of the TV and reduce streaking artifact in the RA [17, 18].

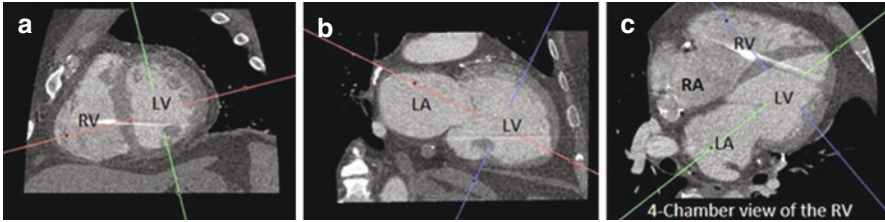
Typically, CT coronary imaging can be obtained in a prospective manner; however, cine images of the tricuspid valve and full RV functional assessments require retrospective ECG gating [19]. This method of image acquisition increases the radiation exposure to the patient. Dose modulation techniques and iterative reconstruction should be used and usually mitigate this increased radiation dose received during retrospective ECG gating.

## Assessment of Right Ventricular Size and Function

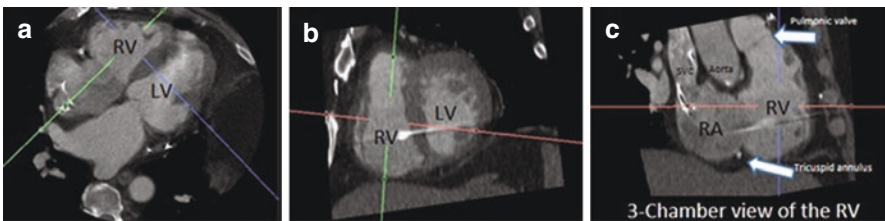
Assessment of RV function with MDCT involves segmentation of the ventricle using several phases of the cardiac cycle, often 10 phases with a 64-slice CT scanner, or 20 phases with dual-source CT scanners. The end-systolic and end-diastolic volumes are determined by evaluating cardiac motion and volume changes by the reader. The endocardium is manually traced to delineate the RV volumes. Stroke volume (SV) is calculated from difference of end-diastolic volume (EDV) and end-systolic volume (ESV). The RV ejection fraction is calculated as the ratio between SV and EDV. Several studies have shown the high accuracy of MDCT for measurement of RV volume and RV ejection fraction compared to CMR [12, 13, 20, 21]. Automated tracing of the RV endocardial borders is available; however, manual corrections of the automated tracing are frequently needed due to complex RV geometry. Multiple views can be reconstructed to view the RV systolic function in four-chamber, two-chamber, and three-chamber views (Figs. 7.1, 7.2, 7.3, and 7.4). Global and regional wall motion abnormalities can also be assessed (Videos 7.1, 7.2, and 7.3). Normative values for the CT-derived cardiac chamber size and function have been reported (Table 7.1) [22].



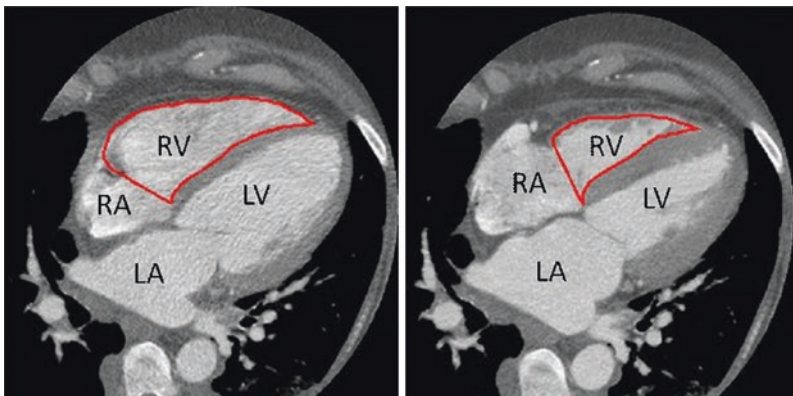
**Fig. 7.1** Creating two-chamber view of the RV. From the short-axis view of the heart (panel **a**) move the center of the planes inside the RV. Then shift the green plane to cross the anterior (free) wall of the RV and the inferior (diaphragmatic) wall of the RV (panel **b**). Then in the modified four-chamber, have the green plane cross the RA (panel **b**). A two-chamber view of the RV will appear (panel **c**). RV right ventricle, RA right atrium, LV left ventricle



**Fig. 7.2** Creating four-chamber view of the LV and RV. From the short-axis view of the heart (panel **a**), place the center planes inside the center of the left ventricle then orientate the red plane to cross the RV at its largest dimension. Next, place the red plane toward the LV apex (panel **b**). This will create a four-chamber view of the right and left ventricle (panel **c**). LV left ventricle, RV right ventricle, LA left atrium, RA right atrium



**Fig. 7.3** Creating three-chamber view of the RV (RV inflow and outflow view). Move the center of the planes to be inside the center of the RV in the four-chamber view (panel **a**), then move the green plane extend along the long axis of the RV into the RVOT (panel **b**), optimize the planes to show both the pulmonic valve and the tricuspid annulus (three-chamber view) (panel **c**). Note the lack of tricuspid/pulmonic valve continuity which makes RVOT obstruction very rare in TV intervention. The area between the pulmonic valve and the tricuspid annulus is near the noncoronary aortic sinus. RV right ventricle, RVOT right ventricular outflow tract, TV tricuspid valve, SVC superior vena cava



**Fig. 7.4** Measuring of the right ventricular volumes using cardiac CT. Tracing the RV endocardial border to assess RV volume for assessment of EDV and ESV to calculate the RV ejection fraction. Notice the difference in the myocardial wall thickness and size of the right atrium in end diastole (left panel) and end systole (right panel). Only one slice is shown; however, ES and ED volumes measurement requires tracing the RV endocardial border on multiple slices. RV right ventricle, LV left ventricle, LA left atrium, RA right atrium, EDV end diastolic volume, ESV end systolic volume, ES end systolic, ED end diastolic

**Table 7.1** Normative values for the CT-derived right ventricle chamber size, volume, and function

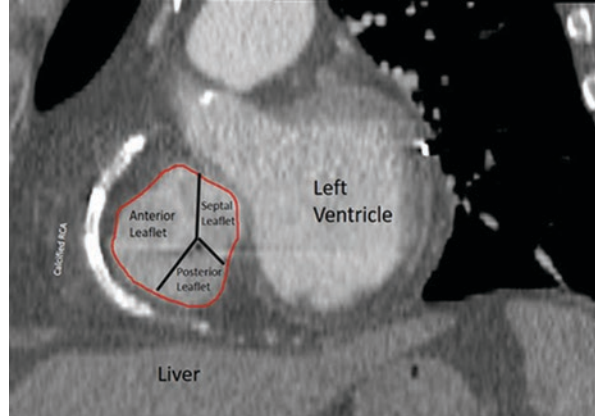
RV dimensions	End-systolic		End-diastolic		Other RV measures	Mean (SD)	95% CI
	Mean (SD)	95% CI	Mean SD	95% CI			
Linear ( <i>n</i> = 103)					Remodeling		
Mid-cavity, septal–medial (mm)	29.6 (5.3)	19.2–40.0	37.0 (5.7)	25.8–48.2	RV free wall thickness	2.4 (0.7)	1.0–3.8
Mid-cavity, anterior–inferior (mm)	57.9 (8.0)	42.2–73.6	72.6 (9.0)	55.0–90.2			
Apical–annular length (mm)	62.0 (8.8)	44.8–79.2	77.7 (10.4)	57.3–98.1			
3D ( <i>n</i> = 85)					Functional measures		
3D volume (ml)	82.1 (29.2)	24.9–139.2	174.9 (48.0)	80.0–269.0	Tricuspid annular excursion (mm)	29.6 (5.3)	19.2–40.0
3D volume index (ml/m <sup>2</sup> )			93.3 (20.3)	53.5–133.1	3D RVEF (%)	57.9 (8.0)	42.2–73.6

RV right ventricle, RVEF right ventricular ejection fraction  
 Reproduced from Lin et al. [22], Copyright 2008, with permission from Elsevier

### *MDCT Assessment of the Tricuspid Annulus*

Functional TR occurs in the setting of right ventricular enlargement and annular dilation. In the assessment of functional TR, it is necessary to have accurate measurement of the TA and leaflet coaptation for possible procedural planning. MDCT TA measurements are taken during diastole at the leaflets most basal attachments (Fig. 7.5). In healthy individuals, the TA is oval shaped and appears approximately 30% longer in the medial to inferolateral direction. The average diameter of TA is 4.0 ± 0.7 cm. The TA area changes by 30% during the cardiac cycle [23–25]. In patients with mild or trace TR, the tricuspid annulus maintains its elliptical shape. In moderate to severe TR, the annulus becomes more circular [26]. As may be expected, the TA area becomes larger with worsening regurgitation and is proportional to TR severity [27]. MDCT can also measure the distance between each leaflet commissure, tethering heights, and tethering angles of each leaflet, each correlating to severity of TR and with prognostic value in patients with severe TR [28]. Tethering height is the distance of commissural displacement into the RV in patients with TR. Tethering area is the area between the annular plane of the TV and the displaced leaflets of the TV. Tethering area greater than 1.6 cm<sup>2</sup> and leaflet coaptation distance greater than 8 mm represent significant tethering and are significant predictors of recurrent TR following TV annuloplasty [29].

**Fig. 7.5** Tricuspid valve annulus with associated tricuspid valve leaflets orientation. Leaflet coaptation lines are marked by the black lines. Note that the largest leaflet is the anterior leaflet. Note the proximity of the RCA (heavily calcified) to the annulus. The red line represents the perimeter of the annulus. RCA, right coronary artery



### *Assessment of Right Ventricular Strain with CT*

Right ventricular strain is a term that is often used to describe the magnitude of right ventricular myocardial deformation. Excessive strain can be caused by acute pulmonary embolism, PHTN, chronic lung disease, or RV infarction. Right ventricular strain has been studied for its prognostic value in patients with heart failure and acute pulmonary embolism and often helps guide management [30, 31]. Both CT and echocardiography can be used to assess RV strain. Right ventricular strain by echocardiography is often measured with either tissue doppler imaging or 2D speckle tracking. Using CT, RV strain is identified using RV-to-LV diameter ratio calculated from a four-chamber image, measuring the maximum distance from the interventricular septum to the endocardium. A normal RV / LV ratio is 0.9–1, moderate RV dilation corresponds to a RV/LV diameter ratio of  $\geq 1.3$  [32, 33]. Additional studies have shown that even in patients with a normal RV/LV ratio, an RV size greater than 45 mm on CT predicts the presence of increased RV strain in patients with acute PE and identifies a subset of patients with poorer overall outcomes [34].




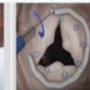
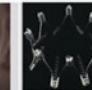



### **Utility of CT in Emerging Transcatheter Tricuspid Valve Interventions**

Traditionally, surgical management of TR had limited scope owing to early data suggesting that isolated left-sided valve repair or replacement led to improvement of TR, and thus, addressing the TV through surgical means was seldom necessary [35]. This was further supported by surgical case series where tricuspid valvulotomy without valve replacement in the setting of recurrent endocarditis led to a low incidence of ensuing treatment-refractory right heart failure [36]. Right ventricular dysfunction, liver cirrhosis, and renal disease are common comorbidities in patients

with severe TR and isolated TV repair or replacement confers an operative mortality on the order of 8–11% [37]. Due to this high perioperative risk and uncertainty surrounding patient selection, surgical volumes have remained low with approximately 5000 cases performed annually [37, 38]. However, more recent appreciation of the morbidity and mortality associated with severe TR has led to expanded surgical indications [39]. This paradigm shift in management has occurred in concert with rapid advances in transcatheter valve repair and replacement devices that offer promising alternatives to surgical approaches.

Multimodality imaging has been essential to successful left-sided transcatheter interventions, and these imaging techniques are being adapted for use during right-sided procedures. While echocardiography is the cornerstone of preoperative and intraoperative imaging, MDCT has proven to be an important adjunctive modality as it offers an accurate assessment of TA and right chamber dimensions, landing zone geometry, caval size assessment, and analyses of possible anatomic impediments to intervention [40]. Two-dimensional (2D) echo and transesophageal echocardiography may provide incomplete assessments of right-sided cardiac structures owing to the unique geometry of the right ventricle, relative anterior positioning, and potential for acoustic shadowing in certain patient populations. MDCT is not bound by these restrictions and offers high-fidelity volumetric assessments via planimetered axial slices. Compared with CMR, MDCT offers superior spatial resolution and comparable chamber quantification when retrospective ECG-gated protocols are employed [41]. Lastly, CT data can be employed in 3D printing software applications to recreate the tricuspid valve apparatus as an adjunct to intervention planning [42].

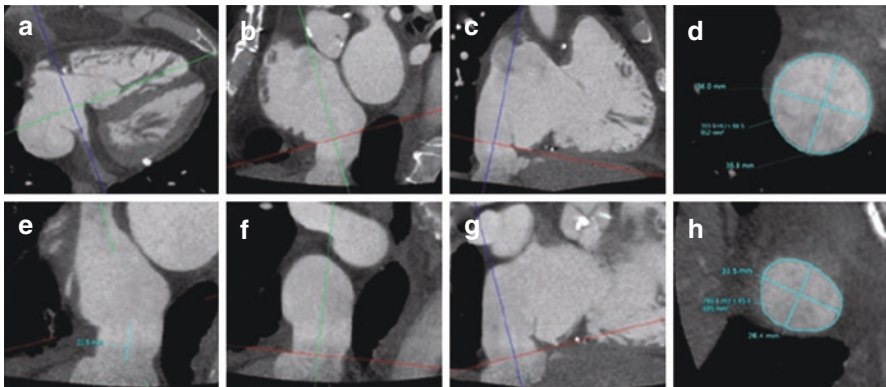
Several transcatheter tricuspid valve repair and replacement devices have been developed and are in various phases of clinical testing. Broadly speaking, these systems target coaptation, annular reduction, leaflet edge-to-edge repair, heterotopic caval valve implantation, and orthotopic valve replacement (Fig. 7.6) [43, 44]. The complex and dynamic nature of the tricuspid valve apparatus and neighboring critical structures demand the high spatial resolution imaging afforded by CT. These anatomic considerations influence the choice in transcatheter device. In approximately two-thirds of patients with significant TR, the right coronary artery (RCA)

	A	B	C	D	E	F	G	H
Device Name	MitraClip	Trialign	TriCinch	CardioBand	Millipede	FORMA Repair System	Caval valve implantation	TRAIPTA
Device Image								
Description	Bicuspidisation of the TV by plicating	Bicuspidisation of the TV by plicating	Bicuspidisation of the TV by cinching	direct annuloplasty device	Complete semi rigid ring	Spacer to occupy the regurgitant orifice area	caval valve implantation in vena cava	Pericardial circumferential device
Access	Transfemoral	Transjugular	Transfemoral	Transfemoral	Transfemoral	Transsubclavian	Transjugular/transfemoral	Transjugular/transfemoral

**Fig. 7.6** Major categories of transcatheter tricuspid valve repair technologies including direct suture annuloplasty, direct ring annuloplasty, indirect annuloplasty, coaptation enhancement, and valve replacement. TV tricuspid valve. (Reprinted with permission from Kuwata et al. [44])



courses within the atrioventricular groove adjacent to the anterior and posterior regions of the TA. In the remaining population, the RCA either courses superior to the tricuspid valve or crosses the horizontal plane of the TA [45]. The mean horizontal distance from the annulus to the RCA at the level of the anterior and posterior tricuspid leaflets is 6.8 mm and 2.1 mm, respectively [46]. The close proximity of RCA to the annulus poses a risk of coronary impingement and acute ischemia, particularly with the deployment annular reduction devices and when the RCA courses <2.0 mm from the annular ring [45]. As the noncoronary sinus of Valsalva is adjacent to the anteroseptal commissure, there is a risk of aortic perforation should a device be anchored at this level. The His bundle is located approximately 3–5 mm posterior to the anteroseptal commissure adjacent to the TV septal leaflet attachment on the membranous septum posing a risk of conduction block should this region be damaged. The TA sizing is important for plication, annular reduction, and valve replacement systems. Defining RV anatomy including RV apex-tricuspid annular distance is important for proper deployment of spacer devices. Delineating the caval borders is essential for sizing of heterotopic caval implants (Fig. 7.7) [45]. In transcatheter mitral valve replacement, left ventricular outflow obstruction is a feared complication and a major focus in preoperative CT imaging [41]. Unlike the continuity between the aortic valve and anterior leaflet of the mitral valve, the tricuspid and pulmonary valves are separated by a ventriculo-infundibular fold. This separation minimizes the risk of neo-right ventricular outflow obstruction during tricuspid valve replacement [41]. While no established imaging guidelines exist,



**Fig. 7.7** Multi-planar CT reconstructions planes for assessment of the IVC dimensions prior to heterotopic caval implantation. (a) Orthogonal axial views of the right ventricular apex and the coronary sinus. (b) Single-oblique sagittal and coronal (c) views, aligned along the transition of right atrium and inferior vena cava parallel to the basal part of the coronary sinus to reconstruct a double-oblique transverse plane of the IVC at the entrance into the right atrium (d). Axial reconstructions positioned at the lower level of the IVC. The distance between the IVC at that point and the first hepatic vein can be measured (e). Using the single-oblique sagittal (f) and coronal (g) views, a double-oblique transverse plane of the IVC can be reconstructed to measure the maximal and minimal diameter, perimeter and area (h). IVC inferior vena cava. (Reprinted by permission of Oxford University Press from van Rosendaal et al. [45])

device-specific CT imaging considerations are summarized in Table 7.2 and described in detail below [40]. Of note, interventions employing leaflet edge-to-edge repair devices such as Mitral Clip (Abbott, Abbott Park, IL) are heavily reliant on echocardiography and CT has a limited role in the preoperative planning.

### ***CT Imaging of Transcatheter Spacer Devices***

Spacer devices, such as the Forma Repair System (Edwards Lifesciences, Irvine, CA), occupy the TV regurgitant orifice area to increase native leaflet coaptation, thereby reducing regurgitant volume (see Figs. 7.6 and 7.8) [47]. This particular device is a foam-filled polymer balloon spacer that is advanced via the left subclavian or axillary vein and placed through the TA over a rail that is subsequently anchored at the septal portion of the right ventricular apex. As detailed in early feasibility studies, ECG-gated MDCT is used to measure TA dimensions, RV diameters, TA–RV apex distance, and subclavian and axillary vein dimensions to ensure compatibility with the device and introducer sheath [47]. The configuration of the subvalvular apparatus including papillary muscles, the moderator band, and positioning of pacing leads (if present) are also assessed. Anchoring targets are selected by drawing a perpendicular line between the tricuspid plane and the RV septal free wall groove in a sagittal MDCT reconstruction perpendicular to the TA (Fig. 7.9). Based on this projection, fluoroscopic angles of coplanarity to the TA are created to assist in preoperative planning. Lastly, CT is also used in follow-up assessments to confirm rail system integrity and positioning [48].

### ***CT Imaging of Transcatheter Annular Reduction Devices***

Annular reduction devices currently under investigation include the TriCinch (4Tech Cardio Ltd., Galway, Ireland), Millipede IRIS (Millipede, Inc., Santa Rosa, CA), Cardioband (Edwards Lifesciences, Irvine, CA), Trialign (MitrAlign, Inc., Tewksbury, MA), and transatrial intrapericardial tricuspid annuloplasty (TRAIPTA) systems (see Fig. 7.6). Computed tomography has an important role in defining the course and distance of the RCA in relationship to the annulus as well as optimizing target positioning through short axis, long two- and four-chamber axis, and volume-rendered reconstruction views [45]. Damage to the RCA with annuloplasty devices is proportional to the distance and course of the RCA with respect to the annulus.

The TriCinch system is comprised of a stainless-steel corkscrew that is anchored in the anterior–posterior TA and linked via a Dacron band to a self-expanding nitinol stent deployed in the IVC between the hepatic and right renal veins. When tension is applied, the septal–lateral annular dimensions are reduced improving the degree of functional TR. First-in-human and feasibility studies have employed CT to identify the optimal anchoring site at the anterior aspect of the TA between the

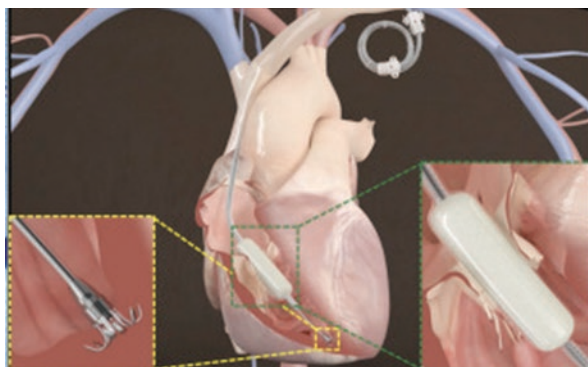
**Table 7.2** Key anatomic considerations during computed tomographic pre-procedural assessment according to anatomic therapeutic target

Device	Anatomic features	Imaging views
Coaptation devices	<ul style="list-style-type: none"> <li>• Tricuspid annular dimensions (anteroposterior and septal-lateral diameter, perimeter, area), midventricular diameter</li> <li>• Distance from the TA to the right ventricular apex</li> <li>• Target anchoring site</li> <li>• Left subclavian and axillary vein</li> </ul>	<ul style="list-style-type: none"> <li>• Short axis of the TA</li> <li>• Long-axis 4-chamber</li> <li>• RV long-axis 2-chamber</li> <li>• Coronal reconstruction</li> </ul>
Annuloplasty devices	<ul style="list-style-type: none"> <li>• Course of the RCA relative to the TA</li> <li>• Distance from RCA to the anterior and posterior tricuspid leaflet insertion</li> <li>• Optimal anchoring target</li> </ul>	<ul style="list-style-type: none"> <li>• Volume-rendered reconstruction, long-axis 2- and 4-chamber, short-axis</li> <li>• Short-axis of the TA and long-axis 4-chamber</li> <li>• Short-axis of the TA</li> </ul>
Heterotopic CAVI	<ul style="list-style-type: none"> <li>• IVC size at the cavoatrial junction and at the level of the first hepatic vein</li> <li>• Distance between the cavoatrial junction and the first hepatic vein</li> </ul>	<ul style="list-style-type: none"> <li>• Double oblique transverse plane of the inferior cavoatrial junction and at the level of the first hepatic vein</li> <li>• Single oblique sagittal plane of the IVC</li> </ul>
Orthotopic TTVR	<ul style="list-style-type: none"> <li>• Tricuspid annular dimensions (anteroposterior and septal-lateral diameters, perimeter, area)</li> <li>• Right internal jugular vein and SVC size</li> <li>• Course of the RCA relative to the TA</li> <li>• Distance from RCA to the anterior and posterior tricuspid leaflet insertion</li> <li>• Risk for ROVT obstruction</li> </ul>	<ul style="list-style-type: none"> <li>• Short axis of the TA</li> <li>• Double oblique transverse plane</li> <li>• Volume-rendered reconstruction, long-axis 2- and 4-chamber, short-axis</li> <li>• Short-axis of the TA and long-axis 4-chamber</li> <li>• Sagittal oblique reconstruction and short axis of the ROVT</li> </ul>

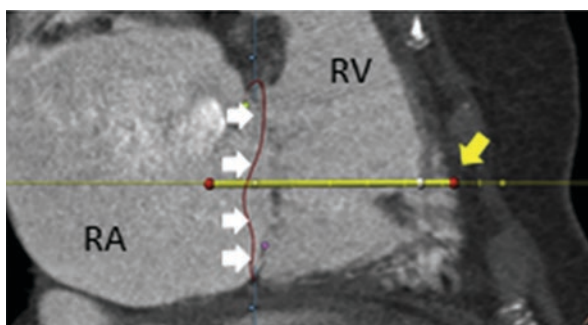
**CAVI** caval valve implantation, **RCA** right coronary artery, **RVOT** right ventricular outflow tract, **SVC** superior vena cava, **TA** tricuspid annulus, **TTVR** transcatheter tricuspid valve replacement

Reprinted from Asmarats et al. [40]. Copyright 2018, with permission from Elsevier

**Fig. 7.8** The FORMA Repair System [47]. A foam-filled polymer balloon spacer that is advanced via the left subclavian vein and placed within the tricuspid annulus anchored at the septal portion of the right ventricular apex. (Reprinted from Campelo-Parada et al. [47], Copyright 2015, with permission from Elsevier)



**Fig. 7.9** Contrast CT-derived reconstructions of the right heart in preparation for FORMA device placement. Sagittal reconstruction delineating the annular plane (white arrows) and the planned anchoring site (yellow arrow). (Reprinted from Perlman et al. [48], Copyright 2017, with permission from Elsevier)



RCA and anterior leaflet hinge point to avoid coronary impingement. CT is also used to ensure appropriate IVC stent sizing (see Fig. 7.7) [49, 50].

The Millipede IRIS transcatheter system consists of a semi-rigid closed annular ring anchored via stainless steel screws on the atrial aspect of the TA. Once placed, adjustable sliding collars are cinched over the collapsible zig-zag nitinol frame to reduce the annular dimension. Initially, the device was surgically placed in the mitral position with the subsequent development of a transcatheter delivery system [51]. The device has since been surgically implanted in the tricuspid valve position and a dedicated transcatheter delivery catheter is currently under development [52]. MDCT is used to define pre- and post-procedure atrial and ventricular volumes as well as annular dimensions (see Fig. 7.6).

The Cardioband system consists of a contraction wire embedded in a polyester sleeve implanted on the atrial side of the TA from the anteroseptal to the septo-posterior commissures via a series of anchors. Once the device is placed, the contraction wire is then cinched, decreasing annular dimensions and reducing TR mimicking the surgical placement of an incomplete annuloplasty ring [53]. Based on initial imaging experience in the mitral space, CT-guided preoperative planning

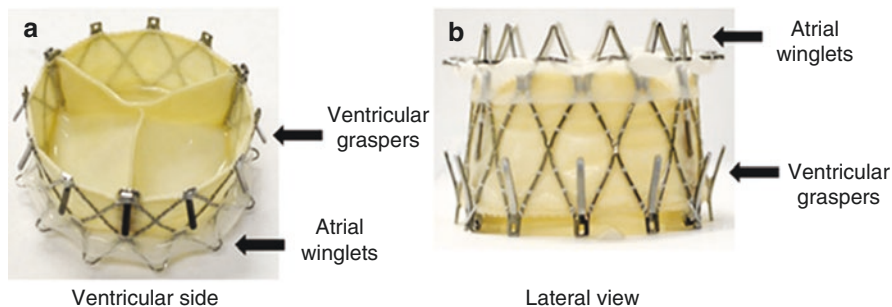
has been adopted in the tricuspid valve for use in assessing annular size and width, planning of fluoroscopic views, and mitigating risk to injury to the RCA [54, 55].

The Trialign system is a transcatheter mimic of the modified Kay procedure that leads to bicuspidization of the tricuspid valve via pledgeted sutures that are subsequently cinched to decrease annular dimensions (see Fig. 7.6). First-in-human and early feasibility studies did not rely heavily on CT imaging; however, CT can be used as an adjunctive modality to define tricuspid anatomy and to localize the RCA course to avoid injury [41, 56, 57].

The TRAIPTA device is an indirect annuloplasty system that consists of a nitinol loop introduced inside the pericardium via the right atrial appendage, and encircling the heart along the atrioventricular groove to reduce annular dimension. Preclinical animal testing studies utilized CT to study the presence of a discrete right atrial lobe to facilitate access, clearly demarcate the atrioventricular groove, and define coronary artery course to assess deployment feasibility [58, 59].

### *CT Imaging of Heterotopic Caval Valve Implantation*

Heterotopic caval valve implantation involves the deployment a bioprosthetic valve in the IVC and/or SVC and has been demonstrated to reduce venous pressure overload and to improve clinical symptoms [60]. Commercially available balloon expandable transcatheter aortic valve replacement (TAVR) valves have also been employed for this purpose with the assistance of pre-implantation caval stents to ensure stable positioning [61]. Compared with patients who have mild-to-moderate TR, those with severe TR can have variably larger IVC diameters that may not be compatible with these repurposed devices [45]. Diameters of the IVC and SVC may reach 35 and 40 mm, respectively, and the mean distance between the inferior cavoatrial junction and the most superior hepatic vein is  $14.1 \pm 5.4$  mm, which is shorter than the width of some existing TAVR valves [62–64]. Thus, tailored bioprosthetic caval implants, that is, TricValve (P&F Products & Features Vertriebs GmbH, Vienna, Austria), have been developed. With these systems, CT plays an important role in caval dimension assessments to assist in prosthetic device customization, if needed, and to avoid complications such as hepatic vein obstruction or device embolization. Necessary imaging information includes obtaining IVC maximal and minimal diameter, perimeter, and area at the cavoatrial junction and at the level of the first hepatic vein as well as the distance between these two anatomical landmarks during mid-diastole (see Fig. 7.7). In the SVC, the diameter of the vein is measured at the superior cavoatrial junction. These dimensions can be obtained via double-oblique transverse and single-oblique sagittal reconstructions at these three respective anatomical positions [45].



**Fig. 7.10** NaviGate-valved stent (a) ventricular side and (b) lateral view showing nitinol frame with atrial winglets and ventricular graspers to secure positioning. (Reprinted with permission from Navia et al. [67])

### ***CT Imaging of Orthotopic Transcatheter Tricuspid Valve Implantation***

Total transcatheter bioprosthetic valve replacement represents an exciting evolution in the management of structural heart disease. For the tricuspid valve, this option had previously been limited to patients who had a prior surgical TV repair with a ring (valve-in-ring) and those with prior bioprosthetic TV (valve-in-valve) implants for failed TV annuloplasty and degenerative bioprosthetic valves, respectively. Cross-sectional imaging with CT has been variably used in these procedures [65, 66]. This area is rapidly evolving with the advent of dedicated fully orthotopic transcatheter tricuspid valve replacement options, that is, Navigate (NaviGate Cardiac Structures, Lake Forest, CA). This device consists of a self-expanding tapered nitinol stent with atrial winglets and ventricular graspers to allow for secure anchoring in the tricuspid annulus (Fig. 7.10). First-in-human studies detail the importance of CT in the pre- and postoperative assessments [67]. Four-dimensional (respiration-correlated) CT provides a phase-resolved visualization of tissue motion, effectively providing 3D cine imaging. This can be used to create a 3D printing model of right heart structures to simulate procedural implantation. As with other transcatheter devices, CT is used to assess chamber quantification, tricuspid annulus, and vascular assess structures. Similar to heterotopic caval devices, CT image acquisition may include short axis views of the TA and RVOT, long-axis two- and four-chamber views, volume-rendered reconstructions, and sagittal- and double-oblique reconstructions (see Figs. 7.1, 7.2, and 7.3). Multiple additional devices are in development and various stages of clinical testing [40, 43].

## References

1. Stuge O, Liddicoat J. Emerging opportunities for cardiac surgeons within structural heart disease. *J Thorac Cardiovasc Surg.* 2006;132(6):1258–61.
2. Agricola E, Stella S, Gullace M, Ingallina G, D’Amato R, Slavich M, et al. Impact of functional tricuspid regurgitation on heart failure and death in patients with functional mitral regurgitation and left ventricular dysfunction. *Eur J Heart Fail.* 2012;14(8):902–8.
3. Topilsky Y, Nkomo VT, Vatury O, Michelena HI, Letourneau T, Suri RM, et al. Clinical outcome of isolated tricuspid regurgitation. *JACC Cardiovasc Imaging.* 2014;7(12):1185–94.
4. Topilsky Y, Maltais S, Medina Inojosa J, Oguz D, Michelena H, Maalouf J, et al. Burden of tricuspid regurgitation in patients diagnosed in the community setting. *JACC Cardiovasc Imaging.* 2019;12(3):433–42.
5. Nath J, Foster E, Heidenreich PA. Impact of tricuspid regurgitation on long-term survival. *J Am Coll Cardiol.* 2004;43(3):405–9.
6. Wijeratne DT, Lajkosz K, Brogly SB, Lougheed MD, Jiang L, Housin A, et al. Increasing incidence and prevalence of world health organization groups 1 to 4 pulmonary hypertension: a population-based cohort study in Ontario, Canada. *Circ Cardiovasc Qual Outcomes.* 2018;11(2):e003973.
7. Gilboa SM, Devine OJ, Kucik JE, Oster ME, Riehle-Colarusso T, Nembhard WN, et al. Congenital heart defects in the United States: estimating the magnitude of the affected population in 2010. *Circulation.* 2016;134(2):101–9.
8. Iglesias-Garriz I, Olalla-Gómez C, Garrote C, López-Benito M, Martín J, Alonso D, et al. Contribution of right ventricular dysfunction to heart failure mortality: a meta-analysis. *Rev Cardiovasc Med.* 2012;13(2–3):e62–9.
9. Prins KW, Rose L, Archer SL, Pritzker M, Weir EK, Olson MD, et al. Clinical determinants and prognostic implications of right ventricular dysfunction in pulmonary hypertension caused by chronic lung disease. *J Am Heart Assoc.* 2019;8(2):e011464.
10. Chorin E, Rozenbaum Z, Topilsky Y, Konigstein M, Ziv-Baran T, Richert E, et al. Tricuspid regurgitation and long-term clinical outcomes. *Eur Heart J Cardiovasc Imaging.* 2020;21(2):157–65.
11. Lin E, Alessio A. What are the basic concepts of temporal, contrast, and spatial resolution in cardiac CT? *J Cardiovasc Comput Tomogr.* 2009;3(6):403–8.
12. Lewis MA, Pascoal A, Keevil SF, Lewis CA. Selecting a CT scanner for cardiac imaging: the heart of the matter. *Br J Radiol.* 2016;89(1065):20160376.
13. Fuchs A, Kuhl JT, Lonborg J, Engstrom T, Vejstrup N, Kober L, et al. Automated assessment of heart chamber volumes and function in patients with previous myocardial infarction using multidetector computed tomography. *J Cardiovasc Comput Tomogr.* 2012;6(5):325–34.
14. Fu H, Wang X, Diao K, Huang S, Liu H, Gao Y, et al. CT compared to MRI for functional evaluation of the right ventricle: a systematic review and meta-analysis. *Eur Radiol.* 2019;29(12):6816–28.
15. Taylor AJ, Cerqueira M, Hodgson JM, Mark D, Min J, O’Gara P, et al. ACCF/SCCT/ACR/AHA/ASE/ASNC/NASCI/SCAI/SCMR 2010 appropriate use criteria for cardiac computed tomography. A report of the American College of Cardiology Foundation Appropriate Use Criteria Task Force, the Society of Cardiovascular Computed Tomography, the American College of Radiology, the American Heart Association, the American Society of Echocardiography, the American Society of Nuclear Cardiology, the North American

- Society for Cardiovascular Imaging, the Society for Cardiovascular Angiography and Interventions, and the Society for Cardiovascular Magnetic Resonance. *J Am Coll Cardiol*. 2010;56(22):1864–94.
16. Stocker TJ, Deseive S, Leipsic J, Hadamitzky M, Chen MY, Rubinshtein R, et al. Reduction in radiation exposure in cardiovascular computed tomography imaging: results from the PROspective multicenter registry on radiation dose Estimates of cardiac CT angIOgraphy iN daily practice in 2017 (PROTECTION VI). *Eur Heart J*. 2018;39(41):3715–23.
  17. Hinzpeter R, Eberhard M, Burghard P, Tanner FC, Taramasso M, Manka R, et al. Computed tomography in patients with tricuspid regurgitation prior to transcatheter valve repair: dynamic analysis of the annulus with an individually tailored contrast media protocol. *EuroIntervention*. 2017;12(15):e1828–e36.
  18. Gopalan D. Right heart on multidetector CT. *Br J Radiol*. 2011;84(3):S306–23.
  19. Shah S, Jenkins T, Markowitz A, Gilkeson R, Rajiah P. Multimodal imaging of the tricuspid valve: normal appearance and pathological entities. *Insights Imaging*. 2016;7(5):649–67.
  20. Plumhans C, Muhlenbruch G, Rapae A, Sim KH, Seyfarth T, Gunther RW, et al. Assessment of global right ventricular function on 64-MDCT compared with MRI. *AJR Am J Roentgenol*. 2008;190(5):1358–61.
  21. Maffei E, Messalli G, Martini C, Nieman K, Catalano O, Rossi A, et al. Left and right ventricle assessment with Cardiac CT: validation study vs. Cardiac MR. *Eur Radiol*. 2012;22(5):1041–9.
  22. Lin FY, Devereux RB, Roman MJ, Meng J, Jow VM, Jacobs A, et al. Cardiac chamber volumes, function, and mass as determined by 64-multidetector row computed tomography: mean values among healthy adults free of hypertension and obesity. *JACC Cardiovasc Imaging*. 2008;1(6):782–6.
  23. Tei C, Pilgrim JP, Shah PM, Ormiston JA, Wong M. The tricuspid valve annulus: study of size and motion in normal subjects and in patients with tricuspid regurgitation. *Circulation*. 1982;66(3):665–71.
  24. Tei C, Shah PM, Cherian G, Trim PA, Wong M, Ormiston JA. Echocardiographic evaluation of normal and prolapsed tricuspid valve leaflets. *Am J Cardiol*. 1983;52(7):796–800.
  25. Ton-Nu TT, Levine RA, Handschumacher MD, Dorer DJ, Yosefy C, Fan D, et al. Geometric determinants of functional tricuspid regurgitation: insights from 3-dimensional echocardiography. *Circulation*. 2006;114(2):143–9.
  26. Saremi F, Hassani C, Millan-Nunez V, Sánchez-Quintana D. Imaging evaluation of tricuspid valve: analysis of morphology and function with CT and MRI. *AJR Am J Roentgenol*. 2015;204(5):W531–42.
  27. Nemoto N, Lesser JR, Pedersen WR, Sorajja P, Spinner E, Garberich RF, et al. Pathogenic structural heart changes in early tricuspid regurgitation. *J Thorac Cardiovasc Surg*. 2015;150(2):323–30.
  28. Kabasawa M, Kohno H, Ishizaka T, Ishida K, Funabashi N, Kataoka A, et al. Assessment of functional tricuspid regurgitation using 320-detector-row multislice computed tomography: risk factor analysis for recurrent regurgitation after tricuspid annuloplasty. *J Thorac Cardiovasc Surg*. 2014;147(1):312–20.
  29. Fukuda S, Song JM, Gillinov AM, McCarthy PM, Daimon M, Kongsarepong V, et al. Tricuspid valve tethering predicts residual tricuspid regurgitation after tricuspid annuloplasty. *Circulation*. 2005;111(8):975–9.
  30. Cameli M, Righini FM, Lisi M, Mondillo S. Right ventricular strain as a novel approach to analyze right ventricular performance in patients with heart failure. *Heart Fail Rev*. 2014;19(5):603–10.
  31. Grifoni S, Olivetto I, Cecchini P, Pieralli F, Camaiti A, Santoro G, et al. Short-term clinical outcome of patients with acute pulmonary embolism, normal blood pressure, and echocardiographic right ventricular dysfunction. *Circulation*. 2000;101(24):2817–22.
  32. Wake N, Kumamaru KK, George E, Bedayat A, Ghosh N, Gonzalez Quesada C, et al. Computed tomography and echocardiography in patients with acute pulmonary embolism: part 1: correlation of findings of right ventricular enlargement. *J Thorac Imaging*. 2014;29(1):W1–6.



33. Kumamaru KK, Hunsaker AR, Bedayat A, Soga S, Signorelli J, Adams K, et al. Subjective assessment of right ventricle enlargement from computed tomography pulmonary angiography images. *Int J Cardiovasc Imaging*. 2012;28(4):965–73.
34. Kumamaru KK, George E, Ghosh N, Quesada CG, Wake N, Gerhard-Herman M, et al. Normal ventricular diameter ratio on CT provides adequate assessment for critical right ventricular strain among patients with acute pulmonary embolism. *Int J Cardiovasc Imaging*. 2016;32(7):1153–61.
35. Braunwald NS, Ross J, Morrow AG. Conservative management of tricuspid regurgitation in patients undergoing mitral valve replacement. *Circulation*. 1967;35(4 Suppl):I63–9.
36. Arbulu A, Holmes RJ, Asfaw I. Tricuspid valvectomy without replacement. Twenty years' experience. *J Thorac Cardiovasc Surg*. 1991;102(6):917–22.
37. Zack CJ, Fender EA, Chandrashekar P, Reddy YNV, Bennett CE, Stulak JM, et al. National trends and outcomes in isolated tricuspid valve surgery. *J Am Coll Cardiol*. 2017;70(24):2953–60.
38. Alqahtani F, Berzingi CO, Aljohani S, Hijazi M, Al-Hallak A, Alkhouli M. Contemporary trends in the use and outcomes of surgical treatment of tricuspid regurgitation. *J Am Heart Assoc*. 2017;6(12):e007597.
39. Nishimura RA, Otto CM, Bonow RO, Carabello BA, Erwin JP, Guyton RA, et al. 2014 AHA/ACC guideline for the management of patients with valvular heart disease: a report of the American College of Cardiology/American Heart Association Task Force on Practice Guidelines. *J Thorac Cardiovasc Surg*. 2014;148(1):e1–e132.
40. Asmarats L, Puri R, Latib A, Navia JL, Rodés-Cabau J. Transcatheter tricuspid valve interventions: landscape, challenges, and future directions. *J Am Coll Cardiol*. 2018;71(25):2935–56.
41. Naoum C, Blanke P, Cavalcante JL, Leipsic J. Cardiac computed tomography and magnetic resonance imaging in the evaluation of mitral and tricuspid valve disease: implications for transcatheter interventions. *Circ Cardiovasc Imaging*. 2017;10(3):e005331.
42. O'Neill B, Wang DD, Pantelic M, Song T, Guerrero M, Greenbaum A, et al. Transcatheter caval valve implantation using multimodality imaging: roles of TEE, CT, and 3D printing. *JACC Cardiovasc Imaging*. 2015;8(2):221–5.
43. Curio J, Demir OM, Pagnesi M, Mangieri A, Giannini F, Weisz G, et al. Update on the current landscape of transcatheter options for tricuspid regurgitation treatment. *Interv Cardiol*. 2019;14(2):54–61.
44. Kuwata S, Zuber M, Pozzoli A, Nietlispach F, Tanner F, Masisano F, et al. Tricuspid regurgitation: assessment and new frontiers. *Cardiovasc Med*. 2017;20(9):203–8.
45. van Rosendael PJ, Kamperidis V, Kong WK, van Rosendael AR, van der Kley F, Ajmone Marsan N, et al. Computed tomography for planning transcatheter tricuspid valve therapy. *Eur Heart J*. 2017;38(9):665–74.
46. Ueda A, McCarthy KP, Sánchez-Quintana D, Ho SY. Right atrial appendage and vestibule: further anatomical insights with implications for invasive electrophysiology. *Europace*. 2013;15(5):728–34.
47. Campelo-Parada F, Perlman G, Philippon F, Ye J, Thompson C, Bédard E, et al. First-in-man experience of a novel transcatheter repair system for treating severe tricuspid regurgitation. *J Am Coll Cardiol*. 2015;66(22):2475–83.
48. Perlman G, Praz F, Puri R, Ofek H, Ye J, Philippon F, et al. Transcatheter tricuspid valve repair with a new transcatheter coaptation system for the treatment of severe tricuspid regurgitation: 1-year clinical and echocardiographic results. *JACC Cardiovasc Interv*. 2017;10(19):1994–2003.
49. Latib A, Ruparelina N, Bijuklic K, De Marco F, Gatto F, Hansen L, et al. First-in-man transcatheter mitral valve-in-ring implantation with a repositionable and retrievable aortic valve prosthesis. *EuroIntervention*. 2016;11(10):1148–52.
50. Early feasibility study of the percutaneous 4tech trinch coil tricuspid valve repair system. [ClinicalTrials.gov](https://clinicaltrials.gov/ct2/show/study/NCT03632967) Identifier: NCT03632967. Accessed 6 Nov 2019.
51. Rogers JH, Boyd WD, Smith TW, Bolling SF. Early experience with Millipede IRIS transcatheter mitral annuloplasty. *Ann Cardiothorac Surg*. 2018;7(6):780–6.

52. Rogers J. Millipede ring for the tricuspid valve. Presented at transcatheter cardiovascular therapeutics 2017; Denver, CO.
53. Kuwata S, Taramasso M, Nietlispach F, Maisano F. Transcatheter tricuspid valve repair toward a surgical standard: first-in-man report of direct annuloplasty with a cardioband device to treat severe functional tricuspid regurgitation. *Eur Heart J*. 2017;38(16):1261.
54. Maisano F, Taramasso M, Nickenig G, Hammerstingl C, Vahanian A, Messika-Zeitoun D, et al. Cardioband, a transcatheter surgical-like direct mitral valve annuloplasty system: early results of the feasibility trial. *Eur Heart J*. 2016;37(10):817–25.
55. Nickenig G. TRI-REPAIR: 30-day outcomes of transcatheter tricuspid valve repair in patients with severe secondary tricuspid regurgitation. Presented at: transcatheter cardiovascular therapeutics 2017; Denver, CO.
56. Hahn RT, Meduri CU, Davidson CJ, Lim S, Nazif TM, Ricciardi MJ, et al. Early feasibility study of a transcatheter tricuspid valve annuloplasty: scout trial 30-day results. *J Am Coll Cardiol*. 2017;69(14):1795–806.
57. Schofer J, Bijuklic K, Tiburtius C, Hansen L, Groothuis A, Hahn RT. First-in-human transcatheter tricuspid valve repair in a patient with severely regurgitant tricuspid valve. *J Am Coll Cardiol*. 2015;65(12):1190–5.
58. Rogers T, Ratnayaka K, Sonmez M, Franson DN, Schenke WH, Mazal JR, et al. Transatrial intrapericardial tricuspid annuloplasty. *JACC Cardiovasc Interv*. 2015;8(3):483–91.
59. Rogers T. TRAIPTA—an update for 2017. Presented at transcatheter cardiovascular therapeutics 2017; Denver, CO.
60. Lauten A, Figulla HR, Unbehaun A, Fam N, Schofer J, Doenst T, et al. Interventional treatment of severe tricuspid regurgitation: early clinical experience in a multicenter, observational, first-in-man study. *Circ Cardiovasc Interv*. 2018;11(2):e006061.
61. Laule M, Stangl V, Sanad W, Lembcke A, Baumann G, Stangl K. Percutaneous transfemoral management of severe secondary tricuspid regurgitation with Edwards Sapien XT bioprosthesis: first-in-man experience. *J Am Coll Cardiol*. 2013;61(18):1929–31.
62. Díez-Villanueva P, Gutiérrezz-Ibañes E, Cuerpo-Caballero GP, Sanz-Ruiz R, Abeytua M, Soriano J, et al. Direct injury to right coronary artery in patients undergoing tricuspid annuloplasty. *Ann Thorac Surg*. 2014;97(4):1300–5.
63. Lauten A, Ferrari M, Hekmat K, Pfeifer R, Dannberg G, Ragoschke-Schumm A, et al. Heterotopic transcatheter tricuspid valve implantation: first-in-man application of a novel approach to tricuspid regurgitation. *Eur Heart J*. 2011;32(10):1207–13.
64. O'Neill BP, Wheatley G, Bashir R, Edmundowicz D, O'Murchu B, O'Neill WW, et al. Study design and rationale of the heterotopic implantation of the Edwards-Sapien XT transcatheter valve in the inferior Vena cava for the treatment of severe tricuspid regurgitation (HOVER) trial. *Catheter Cardiovasc Interv*. 2016;88(2):287–93.
65. Aboulhosn J, Cabalka AK, Levi DS, Himbert D, Testa L, Latib A, et al. Transcatheter valve-in-ring implantation for the treatment of residual or recurrent tricuspid valve dysfunction after prior surgical repair. *JACC Cardiovasc Interv*. 2017;10(1):53–63.
66. McElhinney DB, Cabalka AK, Aboulhosn JA, Eicken A, Boudjemline Y, Schubert S, et al. Transcatheter tricuspid valve-in-valve implantation for the treatment of dysfunctional surgical bioprosthetic valves: an international, multicenter registry study. *Circulation*. 2016;133(16):1582–93.
67. Navia JL, Kapadia S, Elgharably H, Harb SC, Krishnaswamy A, Unai S, et al. First-in-human implantations of the navigate bioprosthesis in a severely dilated tricuspid annulus and in a failed tricuspid annuloplasty ring. *Circ Cardiovasc Interv*. 2017;10(12):e005840.